Expression of Glut-1 and Glut-3 in untreated oral squamous cell carcinoma compared with FDG accumulation in a PET study

Mei Tian[1], Hong Zhang[1, 2], Yoshiki Nakasone[3], Kenji Mogi[3], Keigo Endo[1]

[1] Department of Nuclear Medicine and Diagnostic Radiology, Gunma University School of Medicine, Maebashi, Gunma, Japan
[2] Department of Medical Imaging, Research Center for Charged Particle Therapy, National Institute of Radiological Sciences, Chiba, Japan
[3] Department of Oral and Maxillofacial Surgery, Gunma University School of Medicine, Gunma, Japan

Abstract. Increased expression of glucose transporter-1 (Glut-1) and glucose transporter-3 (Glut-3) has been reported in many human cancers. The mechanism of glucose entry into oral squamous cell carcinoma (OSCC) remains unclear. In this study we investigated, in untreated human OSCC, the relationship between tumour fluorine-18 fluoro-2-deoxy-D-glucose (FDG) accumulation and the expression of Glut-1 and Glut-3, as well as the association between the expression of Glut-1 and of Glut-3. All patients underwent FDG positron emission tomography (PET) pre-operatively. Standardised uptake values (SUVs) were used for evaluation of tumour FDG uptake. Final diagnoses were established by histology. Immunohistochemical staining results were evaluated according to the percentage (%) of positive area, intensity and staining score. Tumour sections were stained by immunohistochemistry for Glut-1 and Glut-3. Glut-1 immunostaining revealed that 18 (94.7%) of the 19 tumours stained positively, while Glut-3 immunostaining yielded positive findings for 16 (84.2%) tumours. Overall, a relatively low level of agreement (36.8%) in the staining score was observed between Glut-1 and Glut-3 expression. No relationship was found between the staining pattern and tumour differentiation or T grade classification in either Glut-1 or Glut-3 immunostaining. Furthermore, no relationship was found between increased FDG SUV and tumour differentiation, but the former did correlate with T grade. In conclusion, high FDG uptake values were seen in OSCC with overexpression of Glut-1 and Glut-3. However, no significant correlation was found between FDG SUV and Glut-1 or Glut-3 expression.

Mei Tian (✉)
Department of Nuclear Medicine and Diagnostic Radiology,
Gunma University School of Medicine, 3-39-22 Showa-machi,
371-8511 Maebashi, Japan
e-mail: tian@med.gunma-u.ac.jp
Tel.: +81-27-2208401, Fax: +81-27-2208409

Introduction

The introduction of positron emission tomography (PET) with fluorine-18 fluoro-2-deoxy-D-glucose (FDG) has opened up a new field of non-invasive imaging and this technique is now used for initial diagnosis, assessment of disease extension and prognosis, planning and monitoring of treatment and detection of recurrent disease [1]. FDG is a glucose analogue that concentrates in cells that rely upon glucose as an energy source or whose dependence on glucose increases under pathophysiological conditions. Increased glucose uptake is one of the major metabolic changes found in malignant tumours [2, 3]. Malignant tumours usually take up glucose and FDG avidly because of increased membrane glucose transporter and glycolytic enzyme activities in tumour cells [1]. The uptake of glucose and other hexoses by human cells can take place via three mechanisms of transport: passive diffusion, Na^+-dependent glucose transporter and facilitative glucose transporters (Glut). Glut is presented on the membranes of almost all cells and is the main pathway by which glucose enters the cell body [4]. Thirteen members of the family of facilitative sugar transporters (Glut-1 to Glut-12 and HMIT; gene name *SLC2A*) are now recognised [5]. These various transporters exhibit different substrate specificities, kinetic properties and tissue expression profiles. Among these subtypes, Glut-1, Glut-3 and Glut-4 have a relatively high affinity for glucose, so they are thought to play an important role in tissues highly dependent on glucose as their energy source [4]. The molecular mechanisms by which increased FDG uptake is sustained, however, are still not

fully understood and are the subject of very intense research efforts.

Several studies have focussed on the expression of glucose transporters and/or hexokinase activity with the aim of defining the role of these two classes of gene in the regulation of FDG uptake [6, 7, 8, 9, 10, 11, 12]. Glut-1 and Glut-3 mRNA was found to be increased in cancers of the oesophagus, colon, pancreas and brain. Glut-1 and Glut-3 protein overexpression was observed in head and neck, lung and pancreatic carcinomas [12, 13, 14], but Glut-4, which largely mediates insulin-dependent glucose transporter, was not found to be expressed in studies including head and neck tumours [12]. The correlation between FDG uptake and the expression of Glut in various tumour cells is still under debate. Further study is necessary to correlate increased FDG uptake by tumours with their Glut-1 and Glut-3 expression, which will lead to a better understanding and interpretation of FDG PET imaging. To the best of our knowledge, no immunohistochemical studies have been published on the relationship between Glut-1 and Glut-3 in oral squamous cell carcinoma (OSCC). Furthermore, no correlative clinical study has been reported regarding the relationship between FDG accumulation and immunohistochemical expression of Glut-1 and Glut-3 in OSCC. In this study, we therefore investigated in patients with untreated OSCC the relationship between tumour FDG accumulation and the expression of Glut-1 and Glut-3, as well as the association between the expression of Glut-1 and of Glut-3.

Materials and methods

Patients. This study was performed on 19 patients (11 male and 8 female, age range 40–78 years) with OSCC who underwent preoperative FDG-PET imaging between June 1999 and January 2002. Another four patients without an appropriate surgical specimen for immunohistochemical evaluation were excluded from this study. The clinical staging was based on the International Union Against Cancer TNM classification [15]. FDG PET and computed tomography (CT) or magnetic resonance imaging (MRI) studies were performed on all patients before treatment. Surgical resection or biopsy confirmed the histological diagnosis. Eleven patients had well-differentiated OSCCs, and the remaining eight patients had moderately differentiated OSCCs. None of the patients had insulin-dependent diabetes, and in all patients the serum glucose level just before FDG injection was less than 100 mg/dl. Informed consent was obtained from all patients participating in this study and the study protocols were approved by the Institutional Review Board of our institute.

FDG PET study. ^{18}F-FDG was synthesised by the Hamacher method [16]. FDG PET studies were performed using a SET 2400 W PET scanner (Shimazu Corporation, Kyoto, Japan) with a 59.5-cm transaxial field of view and a 20-cm axial field of view, which produced 63 image planes, spaced 3.125 mm apart. Transaxial spatial resolution was 4.2 mm full-width at half-maximum (FWHM) at the centre of the field of view, and axial resolution

was 5.0 mm FWHM [17]. A whole-body image was obtained by the simultaneous emission-transmission method with a rotating external source, starting at 60 min after the injection of 185–370 MBq of FDG and using the multiple-bed position technique. Four to five bed positions from the head to the thigh were imaged for 8 min per bed position. Patients fasted for at least 4 h before FDG injection.

Attenuation-corrected transaxial images with FDG were reconstructed by the ordered subsets expectation maximisation (OSEM) algorithm into a 128×128 matrix with pixel dimensions of 4.0 mm in a plane and 3.125 mm axially. Finally, three consecutive slices were added to generate a transaxial image slice 9.8 mm thick for visual interpretation and quantitative analysis by using the standardised uptake value (SUV) [10]. Coronal image slices 9.8 mm thick were also reconstructed from attenuation-corrected transaxial images.

Transaxial and coronal FDG PET images were prospectively interpreted visually by two nuclear physicians in conjunction with CT or MRI until a consensus was reached. Regions of interest (ROIs) were used to evaluate the FDG uptake in segments, with a 4×4 pixels square, including the area of highest activity but not covering the entire tumour. The SUV was defined as the maximum radioactivity in the ROI divided by the injected radioactivity normalised to the body weight.

CT/MRI. CT scan was performed using a Hi-speed helical CT scanner and a LightSpeed QX/I scanner (GE Medical Systems, Milwaukee, WI, USA). Plain axial CT images of 5-mm-thick slices were obtained from the infraorbital plane to hyoid bone. After bolus administration of contrast material, 5-mm-thick slice images were scanned from the infraorbital plane to the supraclavicular region including whole cervical lymph nodes around the sternocleidomastoid muscle.

MR images were obtained using a head coil and a neck coil with the patient in the supine position. MRI was performed with 1.5-T Signa Horizon LX (GE Medical Systems, Milwaukee, WI, USA) and 1.5-T Magnetom Symphony (Siemens Medical Systems, Erlangen, Germany). Transaxial T1-weighted [500–600/10–15 (repetition time, ms/echo time, ms)] and T2-weighted (3,000–5,000/90–100) spin-echo images were obtained before the administration of contrast material. After the first examination, contrast-enhanced T1-weighted images were obtained. Fat saturation was added to T2-weighted images and T1-weighted images after the administration of 0.2 ml/kg of gadodiamide hydrate (Omniscan, Daiichi Seiyaku, Tokyo, Japan) in the case of invasion of adjacent fat tissue.

Histological examination. All patients underwent surgical resection or biopsy within 2 weeks following the PET and CT/MRI studies. Specimens were immediately immersed in 10% formalin solution and processed according to the standard method as paraffin-embedded tissue blocks. Tissue specimens that showed the highest FDG accumulation on PET imaging were used for immunohistochemical staining [14]. Three or more paraffin sections per patients were processed for Glut-1 and Glut-3 immunostaining. Anti-Glut-1 and anti-Glut-3 (Chemicon International Inc., Temecula, CA) are rabbit polyclonal antibodies (sera) generated against 12-amino acid synthetic peptides corresponding to the COOH terminus of human Glut-1 [18] and Glut-3 [19]. The most strongly stained specimen was used for immunostaining analysis. The labelled streptavidin biotin (LSAB) kit (DAKO, Carpinteria, CA) was used for the staining method. All the staining procedures were carried out at room temperature. Sections of 4 μm were cut from the paraffin-embed-

Table 1. Evaluation of staining results

Positive rate (%)	Intensity			
	Negative	Weak	Moderate	Strong
50–100	0	2	3	4
10–50	0	2	3	3
0–10	0	1	2	2
0	0			

ded tissue blocks and hydrated with xylene and graded alcohols. Antigen retrieval methods were performed on all sections before immunostaining procedures. Sections for both anti-Glut-1 and anti-Glut-3 immunostaining were immersed in 0.01 *M* citrate buffer, pH 6.0, by the microwave method (strong range) for three cycles of 5 min. The sections were washed with phosphate-buffered saline (PBS) after 30 min for cooling. After exposure to a mixture of 0.3% hydrogen peroxide in methanol to quench the endogenous peroxidase activity, the sections were treated with blocking buffer (DAKO, contained 10% normal bovine serum in PBS) to block non-specific protein binding, followed by incubation for anti-Glut-1 (1:1,000 dilution by PBS, pH 7.4) or anti-Glut-3 (1:1,000 dilution by PBS, pH 7.4) antibody as a primary antibody for 90 min at room temperature. Parallel sections were incubated with healthy rabbit IgG (20 µg/ml) as negative controls. In the following step, sections were washed in PBS, and the bound antibody was detected using the DAKO LSAB kit with diaminobenzidine (DAB) as chromogen. Finally, sections were counterstained with haematoxylin, dehydrated and mounted. Positive controls for Glut-1 were red blood cells present in each section; for Glut-3, positive controls were sections of human testis [20].

Immunohistochemical evaluation. Two experienced physicians who were unaware of the SUVs independently performed immunohistochemical analysis for Glut-1 and Glut-3. Because Glut can be mainly expressed in the cell membrane, the percentage of cells with Glut-1 and Glut-3 membrane staining was estimated, and its presence was interpreted as overexpression [21]. The overall staining result was scored from 0 to 4 according to the intensity and positive rate of staining as shown in Table 1, which was a modification of the scoring system proposed by Aoki et al. [22]. The intensity of the staining was graded as negative, weak, moderate or strong, according to the method of Mueckler et al. [23] and Higashi et al. [14]. The percentage of positively stained cells was categorised using a semiquantitative scale as 0%, 1–10%, 10–50% and 50–100%.

Statistics. SUV, immunohistochemical staining % positive area, intensity and score, tumour differentiation and tumour T grade classification were analysed for each tumour sample using ANOVA, followed by the Pearson correlation coefficient and Wilcoxon signed rank test. Values were expressed as mean ± standard deviation. *P* values of less than 0.05 were considered statistically significant.

Results

Clinical and PET findings

Clinical and FDG PET results are summarised in Table 2. Eight (42%) of the 19 patients had moderately differentiated OSCC, while 11 (58%) had well-differentiated OSCC. According to the TNM classification, 14 patients (74%) had lower T grades (T1 and T2) and five (26%),

Table 2. Patient characteristics, FDG PET imaging and immunostaining results

Patient no.	Age (yr)	Gender	Histological type	TNM classification	Location	FDG SUV	Glut-1			Glut-3		
							%	Intensity	Score	%	Intensity	Score
1	55	M	Mod. diff. SCC	T1N0M0	Tongue	2.90	70	Strong	4	90	Strong	4
2	77	M	Mod. diff. SCC	T2N0M0	Maxilla	4.37	20	Moderate	3	100	Moderate	3
3	66	M	Mod. diff. SCC	T2N0M0	Tongue	2.80	0	Negative	0	80	Weak	2
4	59	M	Mod. diff. SCC	T2N2M0	Oral floor	3.11	100	Weak	2	0	Negative	0
5	64	M	Mod. diff. SCC	T2N0M0	Buccal mucosa	9.30	70	Weak	2	100	Weak	2
6	71	M	Mod. diff. SCC	T3N0M0	Soft palate	9.33	25	Strong	4	100	Moderate	3
7	65	M	Mod. diff. SCC	T4N2M0	Maxilla	5.57	100	Strong	4	100	Weak	2
8	40	F	Mod. diff. SCC	T4NxMx	Gingiva	8.74	100	Moderate	3	100	Moderate	3
9	70	M	Well diff. SCC	T1N0M0	Gingiva	2.40	90	Strong	4	100	Strong	4
10	49	M	Well diff. SCC	T2N1M0	Soft palate	14.10	90	Strong	4	0	Negative	0
11	78	F	Well diff. SCC	T2N0M0	Buccal mucosa	3.40	80	Strong	4	0	Negative	0
12	74	F	Well diff. SCC	T2N0M0	Maxilla	1.36	100	Weak	2	100	Moderate	3
13	44	M	Well diff. SCC	T2N1M0	Tongue	4.55	100	Strong	4	100	Weak	2
14	77	F	Well diff. SCC	T2N0M0	Buccal mucosa	2.73	100	Strong	4	100	Moderate	3
15	69	F	Well diff. SCC	T2N0M0	Gingiva	7.83	90	Strong	4	90	Strong	4
16	75	F	Well diff. SCC	T2N0M0	Tongue	1.51	100	Strong	4	100	Strong	4
17	78	F	Well diff. SCC	T2N0M0	Tongue	4.09	85	Strong	4	100	Moderate	3
18	78	M	Well diff. SCC	T4N1M0	Tongue	7.46	95	Weak	2	100	Strong	4
19	75	F	Well diff. SCC	T4N0M0	Buccal mucosa	9.56	100	Moderate	3	100	Strong	4

Well diff., well differentiated; mod. diff., moderately differentiated; SCC, squamous cell carcinoma; %, percent positively stained cells

Table 3. Expression of Glut-1 and Glut-3 and FDG uptake in OSCC: relationships to tumour differentiation and TNM stage

No.	All 19	Tumour differentiation			TNM stage		
		Moderate 8	Well 11	P	T1+T2 14	T3+T4 5	P
Glut-1, % positive area	79.74±30.71	60.63±40.39	93.64±7.10	0.039	78.21±30.98	84.00±33.05	0.29
Glut-1, intensity	2.26±0.99	1.88±1.13	2.55±0.82	0.064	2.29±1.07	2.20±0.84	0.099
Glut-1, staining score	3.21±1.13	2.75±1.39	3.55±0.82	0.086	3.21±1.25	3.20±0.84	0.14
Glut-3, % positive area	82.11±36.91	83.75±34.62	80.91±40.11	0.66	75.71±41.45	100±0	0.24
Glut-3, intensity	1.79±1.08	1.50±0.93	2.00±1.18	0.63	1.64±1.15	2.20±0.84	0.37
Glut-3, staining score	2.63±1.38	2.38±1.19	2.82±1.54	0.86	2.43±1.51	3.20±0.84	0.35
Tumour SUV	5.53±3.48	5.77±2.93	5.36±3.96	0.61	4.60±3.52	8.13±1.65	0.04

Table 4. Correlation between staining results for Glut-1 and Glut-3 in OSCC: relationships to tumour differentiation and TNM stage

	Moderate	Well	T1+T2	T3+T4	Total
Glut-1 vs. Glut-3					
% positive area	0.29 (0.51)	0.62 (0.04)	0.12 (0.69)	0.99 (0.001)	0.73 (0.77)
Intensity	0.62 (0.11)	0.31 (0.37)	0.34 (0.24)	0.78 (0.13)	0.16 (0.52)
Staining score	0.50 (0.22)	0.31 (0.36)	0.23 (0.43)	0.78 (0.13)	0.12 (0.62)

Values are r (correlation coefficient), with the probability value (P) within parentheses

higher T grades (T3 and T4). Almost all the tumours were easily visualised on FDG-PET images, the exceptions being in patients 12 (SUV=1.36) and 16 (SUV=1.51). Tumour FDG SUV ranged from 1.36 to 14.10, with an average of 5.53±3.48 for all tumours (Table 3). For the moderately differentiated tumours, SUV ranged from 2.80 to 9.33, with a mean of 5.77±2.93. More variable FDG uptake was seen among patients with well-differentiated tumours, in whom the SUV ranged from 1.36 to 14.10 (mean 5.36±3.96). While the mean SUV for the moderately differentiated tumours was higher than that for the well-differentiated tumours, this difference was not statistically significant (P=0.41). Regarding the T grade, tumours with a lower T grade (T1 or T2) showed a more variable FDG SUV, ranging from 1.36 to 14.10, than tumours with a higher T grade (T3 or T4). The mean SUV in tumours with a higher T grade was significantly higher than that in tumours with a lower T grade (8.13±1.65 vs 4.60±3.52, P=0.04) (Table 3).

Immunohistochemical findings

Negative control sections showed no staining with healthy rabbit immunoglobulin G. For the antibody-stained sections, both the proportion of stained cells and the intensity of staining were evaluated and compared, as shown in Table 2.

Glut-1 immunostaining revealed that 18 (94.7%) of the 19 samples showed positive membrane staining, the exception occurring in patient 3. Glut-1 immunostaining showed a positive area of ≥50% in 16 (84.2%) tumours, and 14 (73.7%) tumours were stained with moderate or strong intensity. Glut-3 immunostaining revealed that 16 (84.2%) tumours stained with a positive area ≥50%, of which 12 (63.2%) were stained with strong or moderate intensity. Three of the tumours graded T2 showed no staining with Glut-3 (patients 4, 10 and 11). Overall, a relatively low level of agreement (36.8%) in the staining score was observed between Glut-1 and Glut-3 expression. No relationships were found between staining patterns and either tumour differentiation or T grade classification in both Glut-1 and Glut-3 immunostaining.

Table 3 summarises the relationships of Glut-1 and Glut-3 expression to tumour differentiation and TNM stage. Correlations between moderately and well-differentiated OSCCs and between higher T grade and lower T grade OSCCs were evaluated and compared with respect to the three scales of % positive area, intensity and staining score for Glut-1 and Glut-3. High values were found on each of the scales for both Glut-1 and Glut-3 staining. The positive area on Glut-1 staining was significantly higher in well-differentiated OSCCs (93.64%±7.10%) than in moderately differentiated OSCCs (60.63%±40.39%) (P=0.039). This was the only significant difference observed with respect to the above three scales. In addition, as shown in Table 4, the % positive area on Glut-1 staining showed a significant correlation (r=0.62, P=0.04) with Glut-3 expression in well-differentiated OSCCs, and a strong positive correlation with Glut-3 expression in OSCCs of higher tumour grade (T3+T4) (r=0.99, P=0.001).
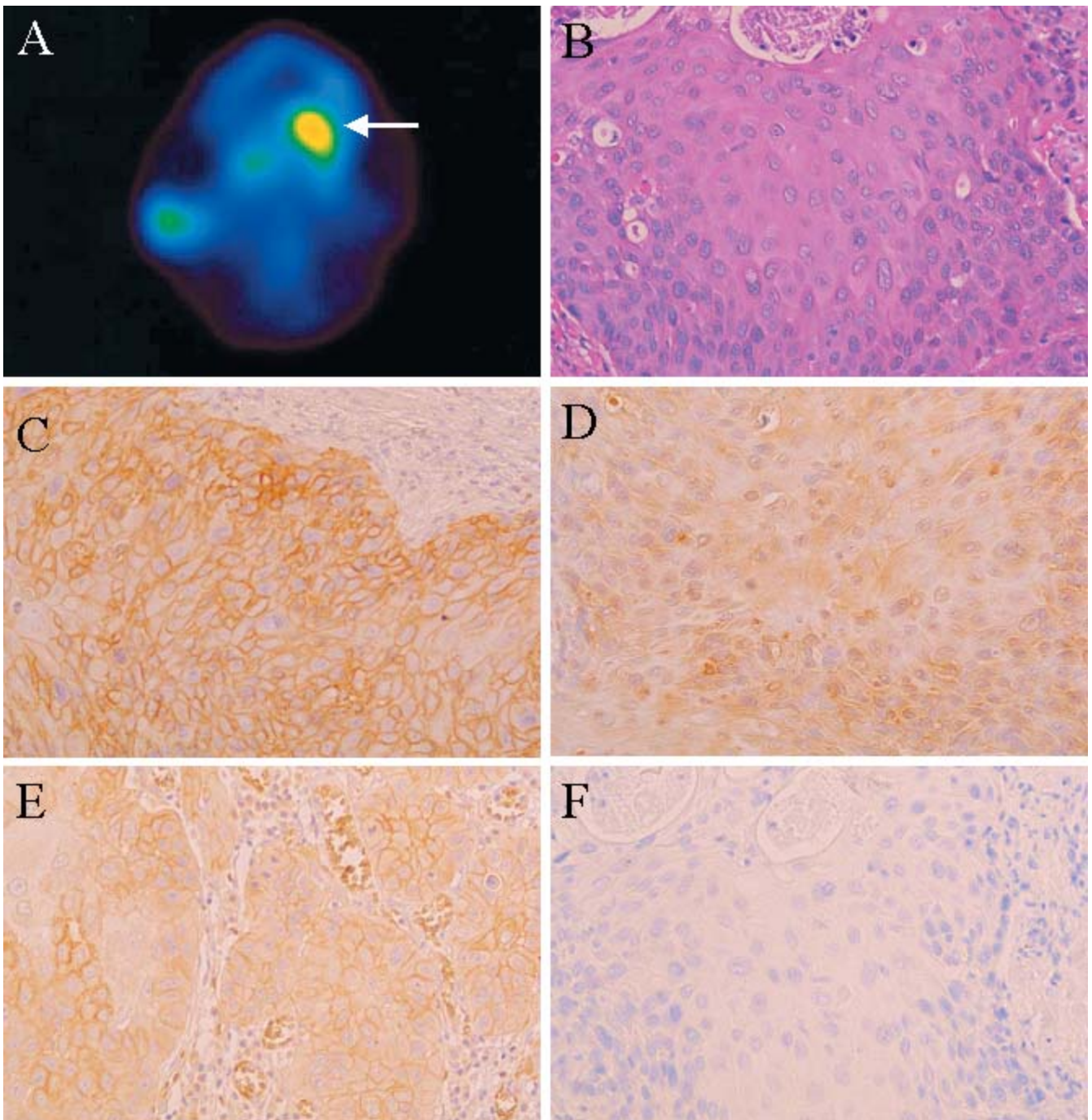
Fig. 1A–F. FDG PET (**A**) shows accumulation (SUV 2.90) in the tongue (*arrow*), and OSCC was confirmed on HE staining (**B**). Immunhistochemical staining of Glut-1 (**C**) and Glut-3 (**D**) shows overexpression of Glut-1 and Glut-3. Expression of Glut-1 is observed mainly in membrane, whereas that of Glut-3 is homogeneous. (**E**) Erythrocytes constantly exhibit intense Glut-1 staining and can be used as internal positive controls. (**F**) The parallel section was incubated with healthy rabbit IgG (20 µg/ml) as a negative control. (Original magnification ×200)

Correlation between FDG accumulation and Glut-1/Glut-3

The results of the statistical comparison between tumour SUV and Glut-1 and Glut-3 immunostaining are shown in Table 5. There was no statistically significant correlation between SUV and Glut-1 or between SUV and Glut-3. All the tumours graded T3+T4 showed a 100% positive area for Glut-3. One representative case, patient 1, is shown in Fig. 1.

Table 5. Correlation between FDG SUV and staining results for Glut-1 and Glut-3 in OSCC: relationships to tumour differentiation and TNM stage

	Moderate	Well	T1+T2	T3+T4	Total
Glut-1 vs SUV					
% positive area	0.003 (0.99)	−0.28 (0.41)	−0.03 (0.91)	−0.48 (0.46)	−0.08 (0.76)
Intensity	−0.25 (0.57)	−0.04 (0.91)	−0.25 (0.40)	−0.41 (0.54)	−0.14 (0.58)
Staining score	−0.25 (0.57)	−0.04 (0.91)	−0.25 (0.40)	−0.41 (0.54)	−0.14 (0.58)
Glut-3 vs SUV					
% positive area	0.40 (0.35)	−0.50 (0.12)	−0.46 (0.10)	0 (1.00)	0.23 (0.34)
Intensity	0.13 (0.77)	−0.39 (0.25)	−0.47 (0.09)	0.38 (0.57)	−0.22 (0.38)
Staining score	0.13 (0.77)	−0.39 (0.25)	−0.47 (0.09)	0.38 (0.57)	−0.22 (0.38)

Values are r (correlation coefficient), with the probability value (P) within parentheses

Discussion

In our study, high FDG SUVs were seen in OSCCs with overexpression of Glut-1 and Glut-3. FDG uptake was increased in OSCCs irrespective of tumour differentiation, but did show a correlation with T grade. FDG is a radiotracer widely used in studies on tissue glucose metabolism with PET. 2-Deoxy-D-glucose and FDG have a lower K_m for transport than their natural counterpart, D-glucose [24]. The transport kinetics of FDG in tumours is largely unknown but some explanation for the in vivo observations regarding tumour FDG uptake in the fasting state and hyperglycaemia can be made on the basis of current knowledge of Glut expression in malignant tissues [25]. Glut-1 and Glut-3 largely mediate basal glucose transport in cancer cells, facilitating the maintenance of glycolytic energy metabolism in cases of limited supply of the substrate in moderately to poorly perfused regions [26]. In cancer-induced malnutrition, overexpression of Glut-1 and Glut-3 may be involved in mechanisms favouring tumour growth at the expense of the host tissues [27]. These subtypes are responsible for transporting the increased amount of glucose and FDG necessary to fulfill the abnormal metabolic requirements of tumour cells. To date, few studies have correlated FDG activity and glucose transporters in human cancers. Although a relationship between Glut-1 expression and FDG uptake has been found for pancreatic cancer and breast cancer [10, 11], no such correlation was seen in non-small cell lung cancer, medullary thyroid cancer or phaeochromocytoma [13,14, 28]. The relationship between FDG accumulation and glucose transporter expression in other human cancers remains unknown.

We consider that the elevated levels of expression of Glut-1 and Glut-3 observed in this study contributed to the accumulation of FDG in OSCCs. With Glut-1 immunostaining, 94.7% of the specimens showed positive membrane staining, and with Glut-3, 16 (84.2%) tumours were positively stained. The prevalence of Glut-1 expression in OSCC was statistically confirmed. This

finding is comparable to the results from a recent study by Kunkel et al. in 118 patients with OSCC [29], in which all OSCC specimens showed Glut-1 expression. A high incidence of Glut-1 expression in SCC cells has also been recognised in lung, skin and head and neck cancers [18, 30, 31]. Differences in Glut expression between tumour cells and normal tissue, and the heterogeneity of Glut-1 expression in different tumours, suggest that such expression may be of biological significance. A correlation was observed between expression of Glut-1 and tumour aggressiveness [32]. For example, Glut-1 expression in colon cancer was found to be correlated with the frequency of lymph node metastases [32].

Mellanen et al. [12] investigated the expression of glucose transporter genes (Glut-1 to Glut-4) in head and neck tumours. Among the 18 patients studied, all 16 SCCs expressed Glut-1 and/or Glut-3 mRNA, while detectable levels of Glut-2 or Glut-4 mRNA were not observed. Histopathological evaluation revealed various grades of differentiation in the SCCs which expressed Glut-1 mRNA at high levels, while Glut-3 mRNA was low in several SCCs. The signals for Glut-1 and Glut-3 mRNA varied markedly in the SCC tumour population, but no clear relationship with the grade of differentiation was found. The high Glut expression observed in some tumours was not associated with amplification or rearrangement of the corresponding genes. The authors suggested that both Glut-1 and Glut-3 are involved in the basal glucose uptake of extracranial head and neck tumours. In the present oral SCC immunohistochemical study, Glut-1 and Glut-3 were predominantly expressed in OSCC tumour cells. We also found that the levels of expression of Glut-1 and Glut-3 varied in the OSCCs of different patients, and there was no significant correlation between FDG SUV and Glut-1 or Glut-3 expression. These results may be partially explained by the differing proportions of tumour and inflammatory cells in different tumours. Mochizuki et al. found that Glut-1 and Glut-3 were highly expressed in malignant tumour and inflammatory tissues. While the level of expression of

Glut-1 was significantly higher in tumour tissue than in inflammatory tissue, that of Glut-3 tended to be higher (non-significant difference) in inflammatory lesions [33]. In the present study, inflammatory cells were found surrounding the OSCC cells in just one patient (no. 5); this patient had a high FDG SUV of 9.30 and showed positive Glut-1 and Glut-3 staining. Changes in Glut expression have also been described in different tissues under various conditions, such as transformation by oncogenes and exposure to insulin or to connective tissue activating peptide-III [34, 35, 36].

Several previous studies have correlated the in vivo evaluation of glucose metabolism with clinical outcome. In a study on head and neck cancer, Minn et al. [37] observed an association between high FDG uptake and poor survival in 37 patients. By contrast, Rege et al. [38] reported improved response to radiation therapy and improved survival in the high-SUV subpopulation in a 12-patient study. Interestingly, in a recent study, a high Glut-1 level and a high FDG SUV predicted shorter survival for patients with OSCC. Glut-1 was found to be a negative biomarker of prognosis and overall survival in patients with OSCC [29]. However, another previous study concluded that immunohistochemical detection of Glut-3 in biopsy specimens of SCC of the larynx is a marker of a poorer prognosis, while Glut1 expression was not associated with survival differences at any cut-off value [39]. It may be concluded that further studies with more patients and using various glucose transporters are required to confirm the roles of glucose transporters in FDG accumulation, and also to determine the prognostic value of FDG SUV and glucose transporters.

In conclusion, in this preliminary study, high FDG uptake values were seen in OSCC with overexpression of Glut-1 and Glut-3. Increased FDG SUV showed no relation to tumour differentiation but did correlate with T grade. However, no significant correlation was found between FDG SUV (at 60 min) and Glut-1 or Glut-3 expression.

References

1. Ak I, Stokkel MP, Pauwels EK. Positron emission tomography with 2-[18F]fluoro-2-deoxy-D-glucose in oncology. Part II. The clinical value in detecting and staging primary tumours. *J Cancer Res Clin Oncol* 2000; 126:560–574.

2. Warburg O, Posenser K, Negelein E. The metabolism of the carcinoma cell. In: *The metabolism of tumors*. New York: Richard R. Smith; 1931:129–169.

3. Isselbacher K. Sugar and amino acid transport by cells in culture—differences between normal and malignant cells. *N Engl J Med* 1972; 286:929–933.

4. Stokkel MP, Linthorst MF, Borm JJ, Taminiau AH, Pauwels EK. A reassessment of bone scintigraphy and commonly tested pretreatment biochemical parameters in newly diagnosed osteosarcoma. *J Cancer Res Clin Oncol* 2002; 128:393–399.

5. Stuart Wood I, Trayhurn P. Glucose transporters (GLUT and SGLT): expanded families of sugar transport proteins. *Br J Nutr* 2003; 89:3–9.

6. Oehr P, Ruhlmann J, Biersack HJ. FDG-PET in clinical oncology: review of the literature and report of one institution's experience. *J Investig Med* 1999; 47:452–461.

7. Yamamoto T, Seino Y, Fukumoto H, Koh G, Yano H, Inagaki N, Yamada Y, Inoue K, Manabe T, Imura H. Over-expression of facilitative glucose transporter genes in human cancer. *Biochem Biophys Res Commun* 1990; 170:223–230.

8. Lindholm P, Minn H, Leskinen-Kallio S, Bergman J, Ruotsalainen U, Joensuu H. Influence of the blood glucose concentration on FDG uptake in cancer—a PET study. *J Nucl Med* 1993; 34:1–6.

9. Brown RS, Leung JY, Fisher SJ, Frey KA, Ethier SP, Wahl RL. Intratumoral distribution of tritiated-FDG in breast carcinoma: correlation between Glut-1 expression and FDG uptake. *J Nucl Med* 1996; 37:1042–1047.

10. Higashi T, Saga T, Nakamoto Y, Ishimori T, Mamede MH, Wada M, Doi R, Hosotani R, Imamura M, Konishi J. Relationship between retention index in dual-phase (18)F-FDG PET, and hexokinase-II and glucose transporter-1 expression in pancreatic cancer. *J Nucl Med* 2002; 43:173–180.

11. Brown RS, Goodman TM, Zasadny KR, Greenson JK, Wahl RL. Expression of hexokinase II and Glut-1 in untreated human breast cancer. *Nucl Med Biol* 2002; 29:443–453.

12. Mellanen P, Minn H, Grenman R, Harkonen P. Expression of glucose transporters in head-and-neck tumors. *Int J Cancer* 1994; 56:622–629.

13. Marom EM, Aloia TA, Moore MB, Hara M, Herndon JE 2nd, Harpole DH Jr, Goodman PC, Patz EF Jr. Correlation of FDG-PET imaging with Glut-1 and Glut-3 expression in early-stage non-small cell lung cancer. *Lung Cancer* 2001; 33:99–107.

14. Higashi T, Tamaki N, Honda T, Torizuka T, Kimura T, Inokuma T, Ohshio G, Hosotani R, Imamura M, Konishi J. Expression of glucose transporters in human pancreatic tumors compared with increased FDG accumulation in PET study. *J Nucl Med* 1997; 38:1337–1344.

15. UICC: TNM classification of malignant tumors, 4th edn. In: Hermanek P, Sobin LH, eds. Berlin Heidelberg New York: Springer, 1987.

16. Hamacher K, Coenen HH, Stocklin G. Efficient stereospecific synthesis of no-carrier-added 2-[18F]-fluoro-2-deoxy-D-glucose using aminopolyether supported nucleophilic substitution. *J Nucl Med* 1986; 27:235–238.

17. Zhang H, Inoue T, Alyafei S, Tian M, Oriuchi N, Endo K. Tumour detectability in 2-dimensional and 3-dimensional positron emission tomography using the SET-2400 W: a phantom study. *Nucl Med Commun* 2001; 22:305–314.

18. Younes M, Lechago LV, Somoano JR, Mosharaf M, Lechago J. Wide expression of the human erythrocyte glucose transporter Glut1 in human cancers. *Cancer Res* 1996; 56:1164–1167.

12

19. Younes M, Lechago LV, Somoano JR, Mosharaf M, Lechago J. Immunohistochemical detection of Glut3 in human tumors and normal tissues. *Anticancer Res* 1997; 17:2747–2750.
20. Younes M, Brown RW, Stephenson M, Gondo M, Cagle PT. Overexpression of Glut1 and Glut3 in stage I nonsmall cell lung carcinoma is associated with poor survival. *Cancer* 1997; 80:1046–1051.
21. Bos R, van Der Hoeven JJ, van Der Wall E, van Der Groep P, van Diest PJ, Comans EF, Joshi U, Semenza GL, Hoekstra OS, Lammertsma AA, Molthoff CF. Biologic correlates of (18)fluorodeoxyglucose uptake in human breast cancer measured by positron emission tomography. *J Clin Oncol* 2002; 20:379–387.
22. Aoki D, Kawakami H, Nozawa S, Udagawa Y, Iizuka R, Hirano H. Differences in lectin binding patterns of normal human endometrium between proliferative and secretory phases. *Histochemistry* 1989; 92:177–184.
23. Mueckler M, Caruso C, Baldwin SA, et al. Sequence and structure of a human glucose transporter. *Science* 1985; 229:941–945.
24. White MK, Bramwell ME, Harris H. Kinetic parameters of hexose transport in hybrids between malignant and nonmalignant cells. *J Cell Sci* 1983; 62:49–80.
25. Lindholm P, Minn H, Leskinen-Kallio S, Bergman J, Ruotsalainen U, Joensuu H. Influence of the blood glucose concentration on FDG uptake in cancer—a PET study. *J Nucl Med* 1993; 34:1–6.
26. Kallinowski F, Schlenger KH, Runkel S, Kloes M, Stohrer M, Okunieff P, Vaupel P. Blood flow, metabolism, cellular microenvironment, and growth rate of human tumor xenografts. *Cancer Res* 1989; 49:3759–3764.
27. Heber D, Byerley LO, Tchekmedyian NS. Hormonal and metabolic abnormalities in the malnourished cancer patient: effects on host-tumor interaction. *JPEN J Parenter Enteral Nutr* 1992; 16 (6 Suppl):60S–64S.
28. Musholt TJ, Musholt PB, Dehdashti F, Moley JF. Evaluation of fluorodeoxyglucose-positron emission tomographic scanning and its association with glucose transporter expression in medullary thyroid carcinoma and pheochromocytoma: a clinical and molecular study. *Surgery* 1997; 122:1049–1060.
29. Kunkel M, Reichert TE, Benz P, Lehr HA, Jeong JH, Wieand S, Bartenstein P, Wagner W, Whiteside TL. Overexpression of Glut-1 and increased glucose metabolism in tumors are associated with a poor prognosis in patients with oral squamous cell carcinoma. *Cancer* 2003; 97:1015–1024.
30. Ito T, Noguchi Y, Satoh S, Hayashi H, Inayama Y, Kitamura H. Expression of facilitative glucose transporter isoforms in lung carcinomas: its relation to histologic type, differentiation grade, and tumor stage. *Mod Pathol* 1998; 11:437–443.
31. Reisser C, Eichhorn K, Herold-Mende C, Born AI, Bannasch P. Expression of facilitative glucose transport proteins during development of squamous cell carcinomas of the head and neck. *Int J Cancer* 1999; 80:194–198.
32. Younes M, Lechago LV, Lechago J. Overexpression of the human erythrocyte glucose transporter occurs as a late event in human colorectal carcinogenesis and is associated with an increased incidence of lymph node metastases. *Clin Cancer Res* 1996; 2:1151–1154.
33. Mochizuki T, Tsukamoto E, Kuge Y, Kanegae K, Zhao S, Hikosaka K, Hosokawa M, Kohanawa M, Tamaki N. FDG uptake and glucose transporter subtype expressions in experimental tumor and inflammation models. *J Nucl Med* 2001; 42:1551–1555.
34. Grobholz R, Hacker HJ, Thorens B, Bannasch P. Reduction in the expression of glucose transporter protein GLUT 2 in preneoplastic and neoplastic hepatic lesions and reexpression of GLUT 1 in late stages of hepatocarcinogenesis. *Cancer Res* 1993; 53:4204–4211.
35. Tai PK, Liao JF, Hossler PA, Castor CW, Carter-Su C. Regulation of glucose transporters by connective tissue activating peptide-III isoforms. *J Biol Chem* 1992; 267:19579–19586.
36. Wagstaff P, Kang HY, Mylott D, Robbins PJ, White MK. Characterization of the avian GLUT1 glucose transporter: differential regulation of GLUT1 and GLUT3 in chicken embryo fibroblasts. *Mol Biol Cell* 1995; 6:1575–1589.
37. Minn H, Lapela M, Klemi PJ, Grenman R, Leskinen S, Lindholm P, Bergman J, Eronen E, Haaparanta M, Joensuu H. Prediction of survival with fluorine-18-fluoro-deoxyglucose and PET in head and neck cancer. *J Nucl Med* 1997; 38:1907–1911.
38. Rege S, Safa AA, Chaiken L, Hoh C, Juillard G, Withers HR. Positron emission tomography: an independent indicator of radiocurability in head and neck carcinomas. *Am J Clin Oncol* 2000; 23:164–169.
39. Baer S, Casaubon L, Schwartz MR, Marcogliese A, Younes M. Glut3 expression in biopsy specimens of laryngeal carcinoma is associated with poor survival. *Laryngoscope* 2002; 112:393–396.